Available online at www.sciencedirect.com
SCIENCE DIRECT
Journal of Molecular Catalysis A: Chemical 243 (2006) 149–157
JOURNAL OF MOLECULAR CATALYSIS A: CHEMICAL
www.elsevier.com/locate/molcata

Characterization and reactivity of Al_2O_3–ZrO_2 supported vanadium oxide catalysts

Komandur V.R. Chary [a,*], Chinthala Praveen Kumar [a], Dhachapally Naresh [a], Thallada Bhaskar [b], Yusaku Sakata [b]

[a] *Catalysis Division, Indian Institute of Chemical Technology, Hyderabad-500 007, India*
[b] *Department of Applied Chemistry, Faculty of Engineering, Okayama University, 3-1-1 Tsushima Naka, 700-8530 Okayama, Japan*

Received 25 March 2005; received in revised form 27 June 2005; accepted 16 July 2005
Available online 23 September 2005

Abstract

Vanadium oxide catalysts with V_2O_5 loadings ranging from 2.5 to 20 wt.% supported on Al_2O_3–ZrO_2 (1:1 wt.%) mixed oxide have been prepared by wet impregnation method. The calcined samples were characterized by X-ray diffraction (XRD), BET surface area, pulse oxygen chemisorption, electron spin resonance (ESR), temperature-programmed reduction (TPR) of H_2, X-ray photoelectron spectroscopy (XPS), and UV–vis diffuse reflectance spectroscopy (UVDRS). The catalytic properties have been evaluated for vapor phase ammoxidation of toluene to benzonitrile. Dispersion of vanadia was determined by the pulse oxygen chemisorption method at 643 K. Vanadia is found to be present in a highly dispersed state at lower loadings and dispersion decreases steadily with increase of vanadia loading. The ESR spectra obtained under ambient conditions shows the presence of V^{4+} in tetrahedral symmetry. The TPR results show a single reduction peak corresponding to $V^{5+} \rightarrow V^{3+}$. XPS results reveal that vanadium is present in a fully oxidized state (+5) in all the samples. The intensity ratio V $2p_{3/2}$/Al $2p_{3/2}$ and V $2p_{3/2}$/Zr $3d_{5/2}$ is found to increase with increase in vanadia loading up to 12.5 wt.% and levels off at higher vanadia loadings. The UV–vis diffuse reflectance spectra indicate the existence of isolated and clusterized tetrahedral (Td) V^{5+} species in all catalysts. Ammoxidation activity increases with vanadia loading up to 12.5 wt.%, which corresponds to monolayer coverage and remains constant at higher vanadia loadings. The catalytic activity in ammoxidation of toluene to benzonitrile has been correlated to the oxygen chemisorption sites.

Keywords: Alumina–zirconia; Vanadia; XRD; ESR; XPS; Ammoxidation

1. Introduction

Supported vanadium oxides have been widely investigated as they represent an important group of catalysts for number of selective oxidation reactions and selective catalytic reduction of NO with NH_3 [1–8]. The surface structures of vanadia supported on oxides such Al_2O_3, SiO_2, ZrO_2 and TiO_2 are quite different from that of bulk vanadia. The efficiency of supported vanadium oxide catalysts mainly depends on the dispersion of the active phase, which in turn can be greatly influenced by the nature of supported oxide, the kind of promoters/additives present and the method of preparation of the catalysts.

In the recent past many studies have been focused related to structural information of the supported vanadium oxides with their catalytic properties [9–14]. Several sophisticated techniques including ESR [15,16], ^{51}V solid state NMR [15,17], electron spectroscopy for chemical analysis [10,11], extended X-ray absorption fine structure (EXAFS) [18,19] and laser Raman spectroscopy [9,11] have been employed to characterize Al_2O_3 and ZrO_2 supported vanadium oxide catalysts in order to understand the relation between catalytic activity and structural aspects. The inherent favorable properties of both alumina and zirconia supports can be explored by the combination of both supports in a mixed oxide. Reports

* Corresponding author. Tel.: +91 40 27193162; fax: +91 40 27160921.
E-mail address: kvrchary@iict.res.in (K.V.R. Chary).

1381-1169/$ – see front matter © 2005 Elsevier B.V. All rights reserved.
doi:10.1016/j.molcata.2005.07.036

in the literature show that the addition of La, Zr and Si modify the alumina surface area and its thermal stability [20]. The combination of Al_2O_3 and ZrO_2 provides greater mechanical strength, which results in improved resistance to attrition [21,22]. In recent years Al_2O_3–ZrO_2-based materials have been employed as catalysts in numerous catalytic applications [13,23,24].

A basic knowledge of the structure–activity relationship observed in heterogeneous catalytic oxidation is of great importance for the development of new catalytic materials and for improving the performance of existing catalysts [25]. To this end, methods such as oxygen chemisorption, XPS studies etc., have been extensively used in recent years to find the active phase dispersion in supported metal oxide systems [10,15,26–28]. Gil-Llambias et al. [27] have reported a linear dependence between XPS intensity ratio of V 2p–Al 2p or Ti 2p peaks and a function of V_2O_5 loading. Similar observations have also been made by Meunier et al. [29].

In the present investigation, we report a systematic study on the characterization of vanadia catalysts supported on Al_2O_3–ZrO_2 by XRD, oxygen chemisorption, ESR, TPR, UV-DRS and XPS measurements. The catalytic properties were evaluated for ammoxidation of toluene to benzonitrile. The purpose of this work is to estimate the dispersion of vanadia supported on Al_2O_3–ZrO_2 binary oxide and also to identify the changes in the structure of vanadium oxide species as a function of an active component loading. The catalytic properties in ammoxidation of toluene were correlated with oxygen chemisorption and other characterization techniques.

2. Experimental

Al_2O_3–ZrO_2 (1:1) mixed oxide support was prepared by co-precipitation method. The requisite quantities of aqueous solutions containing aluminium nitrate hydrate (Merck), zirconyl nitrate hydrate (Merck) and diluted ammonia were continuously stirred for 6 h at 343 K. The precipitation was completed after 4–5 h of stirring at the pH of the solution ≈9. The precipitate thus obtained was filtered, washed several times with demineralized water till it is free from nitrates. The wet cake was dried for 16 h at 383 K and calcined in static air at 773 K for 6 h. The resulting mixed oxide had BET surface area of 163 m^2/g. A series of V_2O_5 catalysts with vanadia loadings ranging from 2.5 to 20 wt.% supported on Al_2O_3–ZrO_2 were prepared by wet impregnation of the support using oxalic acid solution containing requisite amount of ammonium metavanadate (1:2 weight ratio between ammonium metavanadate and oxalic acid). The catalysts were subsequently dried at 383 K for 16 h and calcined in air at 773 K for 6 h.

X-ray diffractograms of V_2O_5/Al_2O_3–ZrO_2 catalysts were recorded on Bruker D-8 diffractometer using graphite filtered Cu Kα radiation (λ = 1.5418 Å).

Oxygen chemisorption was measured by dynamic method on Auto Chem 2910 (Micromeritics, USA) instrument. Prior to adsorption measurements, 0.5 g of the sample was reduced in a flow of hydrogen (50 ml/min) at 643 K for 2 h and flushed out subsequently in a pure He flow (purity 99.995%) for an hour at the same temperature. Oxygen uptake was determined by injecting pulses of oxygen from a calibrated on-line sampling valve into a He stream passing over reduced samples at 643 K. Adsorption was deemed to be complete after at least three successive peaks showed the same area. The BET surface area of the catalyst samples was measured on a Pulse Chemisorb 2700 (Micromeritics) unit by nitrogen physisorption at 77 K.

ESR measurements were recorded at room temperature on a Bruker ESP 300 E (X-band) spectrometer (ν = 9.473 GHz) with 100 kHz modulations. The samples in powder form were loaded in quartz tubes (4 mm internal diameter). A microwave power of 20 mW and modulation amplitude of 4 G was used for each measurement.

TPR experiments were carried out on Auto Chem 2910 instrument. Prior to TPR studies the catalyst sample was pretreated at 673 K for 2 h in flowing hydrocarbon free dry air in order to eliminate the moisture and to ensure complete oxidation. After pretreatment the sample was cooled to room temperature. Carrier gas (5% hydrogen–95% argon) purified through oxy-trap and molecular sieves was allowed to pass over the sample. Temperature was increased from ambient to 1273 K at a heating rate of 10 K/min and the data was recorded simultaneously. The hydrogen consumption values are calculated using GRAMS/32 software.

The UV–vis diffuse reflectance spectra were recorded on a GBC UV–vis Cintra 10_e spectrometer with an integrating sphere reflectance accessory using pellets of 50 mg catalyst sample grounded with 2.5 g of KBr. The KBr was used as diluent and reference material. The accessory is a barium sulphate-coated integrating sphere with light detection by a built-in photomultifier tube attached to the base of the sphere. The sphere is supplied with spectral on reference discs to provide optimal performance across the wavelength range from 200 to 800 nm. The sphere is fitted with 10 mm cell holders and solid sample holders for both reference and a sample positions in order to perform the measurements of reflectance absorbance of samples placed in the rear (reflectance) solid sample holder.

X-ray photoemission spectra were recorded on a KRATOS AXIS 165 equipped with Mg Kα radiation (1253.6 eV) at 75 W apparatus using the Mg Kα anode and a hemispherical analyzer, connected to a five-channel detector. The C 1s line at 284.6 eV was used as an internal standard for the correction of binding energies. The background pressure during the data acquisition was kept below 10^{-10} bar. Spectra were deconvoluted using Sun Solaris based Vision 2 curve resolver. The location and the full width at half maximum (FWHM) for all species were first determined using the spectrum of a pure sample. The location and FWHM of products, which were not obtained as pure species, were adjusted until the

best fit was obtained. Symmetric Gaussian shapes were used in all cases. Binding energies for identical samples were, in general, reproducible to within ±0.1 eV. Calculations of the atomic ratios V/Zr and V/Al were performed by determining the V $2p_{3/2}$, Zr $3d_{5/2}$ and Al $2p_{3/2}$ peak areas, after subtracting the inelastic background and correction of intensities by the respective sensitive factors.

The ammoxidation of toluene to benzonitrile reaction was carried out in a fixed-bed down-flow reactor with 20 mm internal diameter made of Pyrex glass. 0.5 g of the catalyst with a 18–25-mesh size diluted with an equal amount of quartz grains of the same dimensions was charged into the reactor supported on a glass wool bed. In order to minimize the adverse thermal effects, the catalyst particles were diluted to its same volume with quartz grains of similar particle size. Prior to introducing the reactant toluene with a syringe pump (B-Braun perfusor, Germany) the catalyst was reduced at 643 K for 2 h in hydrogen flow (40 ml/min) and then the reactor was fed with toluene, ammonia and air in the molar ratio of 1:13:26. The zone above the catalyst bed was filled-up with quartz glass particles to serve as the preheater. It is heated up to 423 K by way of electrical furnace for adequate vaporization of liquid feed. The reaction products benzonitrile and benzene were analyzed by HP 6890 gas chromatograph equipped with a flame ionization detector (FID) using HP-5 capillary column.

3. Results and discussion

The Al_2O_3–ZrO_2 binary oxide support prepared by co-precipitation method is found to be X-ray amorphous. Different loadings of vanadia supported on Al_2O_3–ZrO_2 catalysts are also found to be amorphous. This observation suggests that deposited vanadia is in well dispersed state on alumina–zirconia support probably in the form of highly active monomeric VO_4 units and two dimensional (V–O–V) structures [30] which seems to be responsible for the ammoxidation of toluene to benzonitrile. XRD also indicates that no compound is formed due to the interaction between V_2O_5 and Al_2O_3 or ZrO_2. The surface area of the catalysts decreases with increasing vanadia content due to blocking of pores with the deposition of vanadia on pore surface of the support (Table 1).

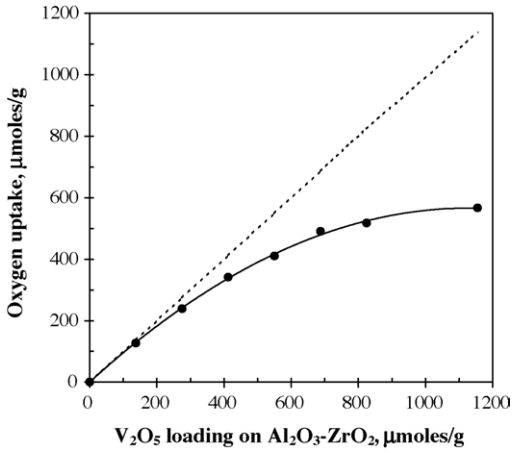

Fig. 1. Oxygen uptake plotted as a function of V_2O_5 loading on Al_2O_3–ZrO_2 support $T_{ads} = T_{red} = 643$ K.

The oxygen uptake plotted as a function of V_2O_5 loading at 643 K is shown in Fig. 1 for vanadia/alumina–zirconia catalysts. The oxygen uptake by alumina–zirconia support under similar conditions was found to be negligible. The oxygen uptakes were found to increase with vanadia loading up to 12.5 wt.% of V_2O_5 and levels off at higher vanadia loadings. This can be attributed to the formation of a vanadium oxide monolayer on alumina–zirconia. The saturation level off of oxygen uptake (Fig. 1) at 12.5 wt.% vanadia loading might be due to the formation of a crystalline vanadia phase. This phase upon pre-reduction with hydrogen does not appreciably chemisorb oxygen. The dashed line in Fig. 1 corresponds to an oxygen atom per a vanadium atom. The dispersion of vanadia can be defined as a fraction of total O atoms titrated (determined from oxygen uptake) to total V atoms present in the sample [15]. A substantial decrease in the dispersion of vanadia is observed with increasing V_2O_5 content in the catalysts. For the same composition of V_2O_5, the dispersion of vanadia supported on mixed alumina–zirconia support was found to be more than that of vanadia supported on simple zirconia [31] and alumina [15] supports.

Table 1
Oxygen uptake, dispersion, oxygen atom site density and surface areas of V_2O_5/Al_2O_3–ZrO_2 catalysts

S. No.	V_2O_5 on Al_2O_3–ZrO_2 (wt.%)	BET surface area ($m^2\ g^{-1}$)	Oxygen uptake[a] ($\mu mol\ g^{-1}$)	Oxygen atom site density ($10^{18}\ m^{-2}$)	Dispersion[b] (O/V)
1	2.50	140	127	1.1	92
2	5.00	128	239	2.3	87
3	7.50	121	341	3.4	83
4	10.0	117	411	4.2	75
5	12.5	114	491	5.2	71
6	15.0	102	518	6.1	63
7	20.0	94	567	7.3	52

[a] T (reduction) = T (adsorption) = 643 K.
[b] Dispersion: fraction of vanadium atoms at the surface assuming $O_{ads}/V_{surf} = 1$.

Table 2
Spin Hamiltonian parameters of V^{4+} in V_2O_5/Al_2O_3–ZrO_2 catalysts

S. No.	V_2O_5 on Al_2O_3–ZrO_2 (wt.%)	$g_\parallel$	$A_\parallel$ (Gauss)	$g_\perp$	$A_\perp$ (Gauss)
1	2.50	1.972	196	1.989	71.0
2	5.00	1.980	177	1.989	64.5
4	10.0	1.988	191	1.992	67.5
5	12.5	1.984	182	1.991	65.3
6	15.0	1.987	176	1.989	64.3
7	20.0	1.986	177	1.989	61.3

Electron spin resonance spectroscopy has been widely used for characterizing supported vanadia catalysts to determine the possible coordination environment i.e., symmetry of vanadium and the effect of support on vanadyl bond strength. The V^{4+} species in the catalysts exhibit clear eight line hyperfine splitting due to interaction between electron spin ($S = +1/2$) and nuclear spin ($I = +7/2$). It can be noticed that the spectra contains a pattern of eight parallel and eight perpendicular hyperfine components, which is a sign of vanadyl ions in axial symmetry. The ESR spectra of calcined V_2O_5/Al_2O_3–ZrO_2 catalysts recorded at ambient temperature are shown in Fig. 2. The spin Hamiltonian parameters such as $g_\parallel$, $A_\parallel$, $g_\perp$ and $A_\perp$ values are given in Table 2. The observed components of g factor show that the g tensor of V^{4+} has axial symmetry. The broadening of ESR spectra at higher loadings of vanadia might be due to the presence of different surface crystalline vanadia. These results further support the vanadia dispersion determined by the oxygen chemisorption method. The high dispersion of vanadia is consistent with the appearance of a well-resolved ESR spectrum in lower vanadia loading samples. The decrease in the intensity of the ESR spectra with increasing of vanadia loading in the catalyst is attributed to spin-spin coupling. The changes in ESR spectral features with vanadia loading might be due to the presence of different vanadia species on Al_2O_3–ZrO_2. The present ESR results are in agreement with our earlier reports [15].

The TPR profiles of bulk V_2O_5 and various V_2O_5/Al_2O_3–ZrO_2 catalysts are shown in Fig. 3. It was found that bulk V_2O_5 exhibited multiple major reduction peaks when reduced in 5% H_2 + 95% Ar up to 1273 K. Koranne et al. [32] and Bosch et al. [33] have reported similar observations, and they have attributed this phenomenon to the following reduction sequence:

$$V_2O_5 \xrightarrow{(1)} V_6O_{13} \xrightarrow{(2)} V_2O_4 \xrightarrow{(3)} V_2O_3$$

The sharp peak at 965 K corresponds to the reduction of V_2O_5 to V_6O_{13} (first peak). The second peak at 1003 K is associated with the reduction of V_6O_{13} to V_2O_4, and the third peak at 1067 K corresponds to V_2O_3 formed by the reduction of V_2O_4.

The TPR profiles of the samples show only a single reduction peak corresponding to $V^{5+} \rightarrow V^{3+}$. It is expected that particle size increases with increase in vanadia loading and the vanadia becomes difficult to reduce due to bulk diffusion limitations. This causes a shift in the TPR peaks to higher

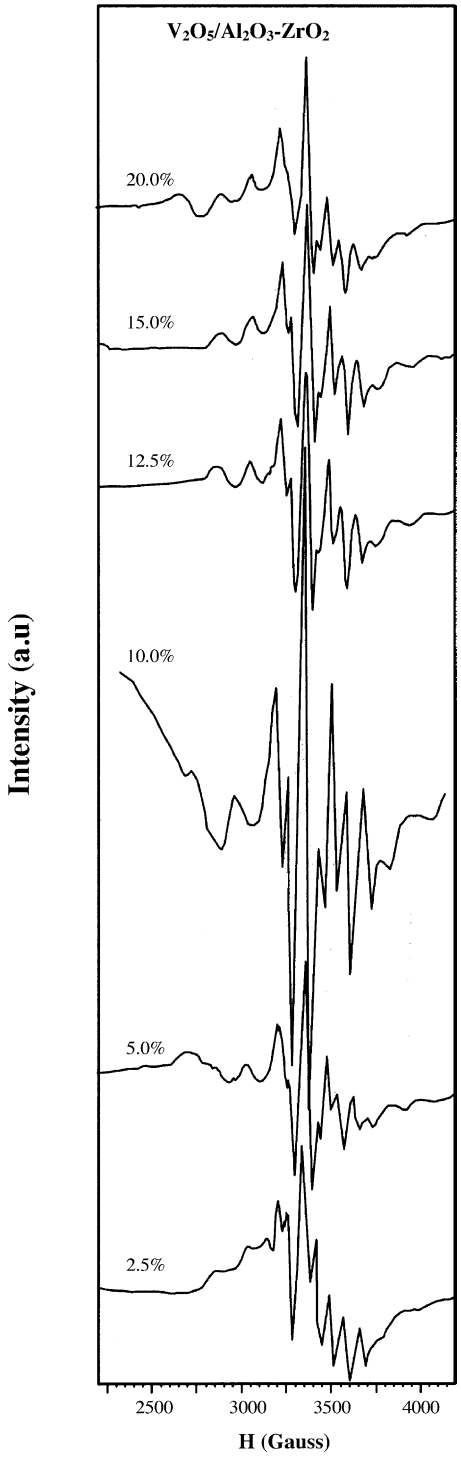

Fig. 2. Electron spin resonance spectra of V_2O_5/Al_2O_3–ZrO_2 catalysts.

temperatures. Thus, the reduction temperature (T_{red}) shifted to higher temperatures (778–814 K) when vanadia loading was increased from 2.5 to 20 wt.% (Table 3). This is an indication of increased particle size of microcrystalline vanadia with higher loadings. It is clear that dispersion decreases when the crystallite size increases, which is in good agreement with the fact that smaller crystallites are reduced faster

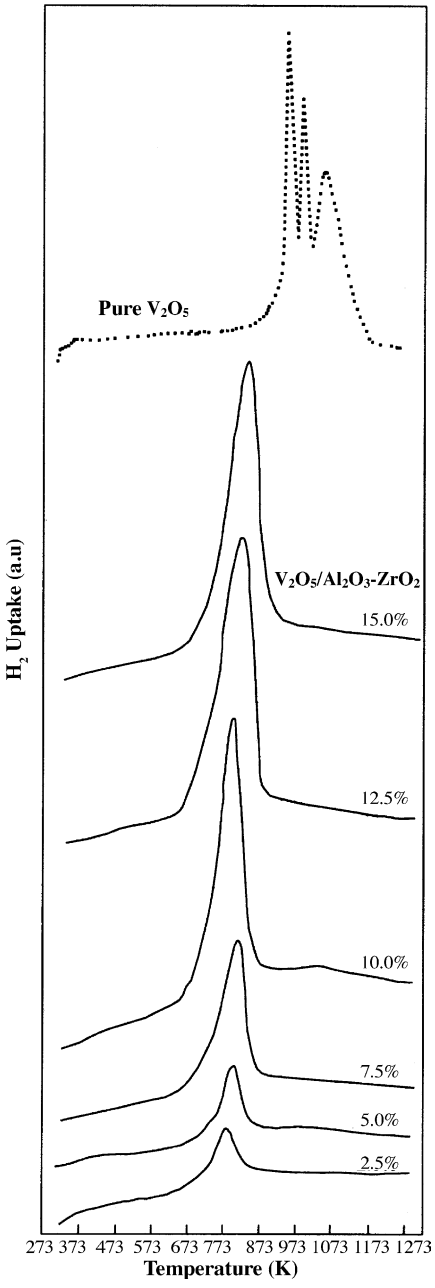

Fig. 3. Temperature-programmed reduction profiles of pure V_2O_5 and V_2O_5/Al_2O_3–ZrO_2 catalysts.

Table 3
Temperature-programmed reduction of V_2O_5/Al_2O_3–ZrO_2 catalysts

S. No.	V_2O_5 on Al_2O_3–ZrO_2 (wt.%)	T_{Red} (K)	H_2 consumption (μmol g^{-1})
1	2.50	778	263
2	5.00	793	544
3	7.50	803	825
4	10.0	788	1071
5	12.5	809	1383
6	15.0	814	1660

than the bigger ones. The shift in reduction temperature indicates that the reducibility of vanadia decreases with loading on Al_2O_3–ZrO_2. The reduction of bulk V_2O_5 occurred at much higher temperatures than Al_2O_3–ZrO_2 supported vanadia due to increased diffusional limitations in bulk V_2O_5 in accordance with the above trend. This is consistent with the work of Koranne et al. [32] and Roozeboom et al. [34]. They have also shown that the supported vanadium oxide catalysts reduce at much lower temperature than bulk vanadia and the reducibility of vanadia is strongly influenced by the kind of support used. Bond et al. [35,36] also reported that the VO_x monolayer species is reduced in a single step from V^{5+} to V^{3+}.

X-ray photoelectron spectroscopy (XPS) is highly surface sensitive technique and considered as one of the best technique for studying the dispersion of V_2O_5 on various supports. The nature of surface species of the V_2O_5/Al_2O_3–ZrO_2 catalysts was investigated by the XPS technique (Figs. 4–7). The photoelectron peaks of O 1s, Zr 3d, Al 2p and V 2p are shown in Figs. 4–7, respectively. The binding energy of O 1s is observed at ~532 eV in Fig. 4. The 1s O profile is due to the overlapping contribution of oxygen from ZrO_2 and Al_2O_3 in the case of mixed Al_2O_3–ZrO_2 support and to ZrO_2, Al_2O_3 and V_2O_5 in the case of the V_2O_5/Al_2O_3–ZrO_2 catalyst samples, respectively. With the increase in vanadia loading there

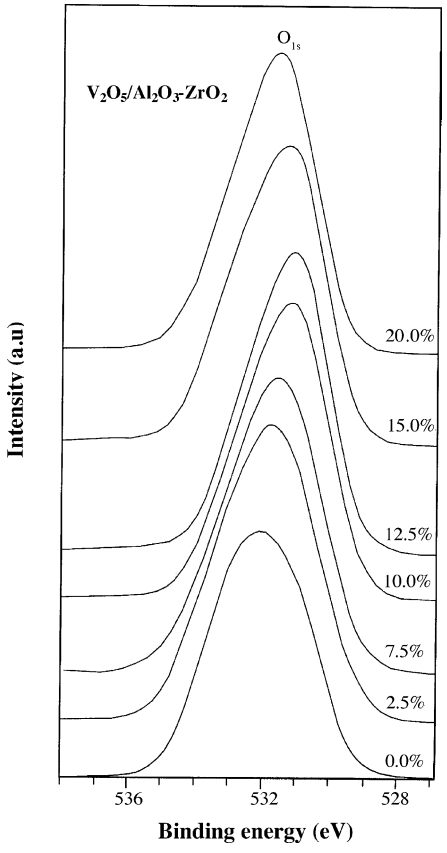

Fig. 4. XPS O 1s binding energy for Al_2O_3–ZrO_2 support and V_2O_5/Al_2O_3–ZrO_2 catalysts.

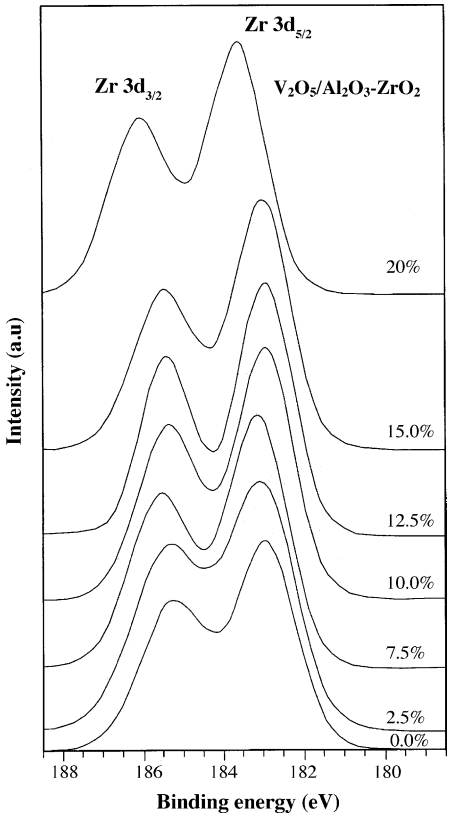

Fig. 5. Zr 3d XPS of the Al_2O_3–ZrO_2 support and V_2O_5/Al_2O_3–ZrO_2 Catalysts.

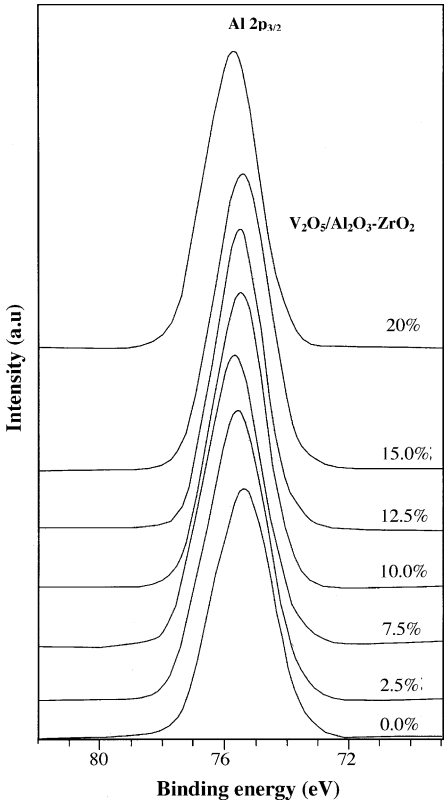

Fig. 6. Al 2p XPS of the Al_2O_3–ZrO_2 support and V_2O_5/Al_2O_3–ZrO_2 catalysts.

is a slight shift in the O 1s B.E values towards lower side. This is due to a contribution from the second O 1s component due to lattice oxygen in the added vanadium phase [37].

Fig. 5 shows the binding energies of Zr photoelectron peaks at ∼182.9 and ∼185.3 eV for Zr $3d_{5/2}$ and Zr $3d_{3/2}$ lines, respectively. The binding energies of Zr $3d_{5/2}$ and its full width half maximum (FWHF) values are shown in Table 4. These values did not change much with different vanadia loadings. The constant FWHM values are around 1.7, implying that only one type of doublet is present. This provides evidence for the presence of a single type of zirconium oxide with an oxidation state of 4+. The intensity of Zr 3d core level spectra does not change much with the increase in vanadia loading. Fig. 6 shows the binding energy of Al 2p photoelectron peak at ∼75.5 eV for Al $2p_{3/2}$, which is in agreement with the values reported in the literature [38]. There is a slight increase in the binding energies of Zr 3d and Al 2p in supported vanadia catalysts. This can be attributed to the strong interactions between the vanadium oxide and support oxides. The binding energies of Al $2p_{3/2}$ and its FWHM values are reported in Table 4. The constant binding energies of Al $2p_{3/2}$ and FWHM values indicate the presence of one type of aluminium oxide with an oxidation state of 3+. The V 2p photoelectron peaks of vanadia catalysts at ∼517.9 and ∼524.2 eV correspond to the V $2p_{3/2}$ and V $2p_{1/2}$ states are shown in Fig. 7. Increasing the vanadia loading does not change in the peak parameters (Table 4), suggesting that only one type of vanadium oxide with +5 oxidation state is present in all the samples. There has been some discussion over the years about the oxidation state of the surface vanadia species

Table 4
Binding energies (eV), FWHM, XPS atomic ratios of O 1s, Zr $3d_{5/2}$ Al $2p_{3/2}$ and V $2p_{3/2}$ for V_2O_5/Al_2O_3–ZrO_2 catalysts

V_2O_5 on Al_2O_3–ZrO_2 (wt.%)	O 1s position	Position and FWHM[a] of Zr $3d_{5/2}$	Position and FWHM of Al $2p_{3/2}$	Position and FWHM of V $2p_{3/2}$	XPS Intensity V 2p/Zr 3d	XPS Intensity V 2p/Al 2p
0	532.1	182.9(1.7)	75.4(2.1)	–	–	–
2.5	532.0	183.2(1.8)	75.6(2.1)	518.1(2.1)	0.234	0.084
7.5	531.7	183.3(1.7)	75.7(1.9)	518.0(1.8)	0.502	0.212
10.0	531.2	182.9(1.7)	75.5(1.9)	517.9(1.7)	0.620	0.244
12.5	530.9	182.9(1.6)	75.5(1.8)	517.8(1.7)	0.765	0.254
15.0	531.3	183.0(1.6)	75.4(1.9)	518.1(1.7)	0.730	0.206
20.0	531.8	183.8(1.5)	75.7(1.9)	518.2(1.8)	0.755	0.232

[a] Parentheses are FWHM values.

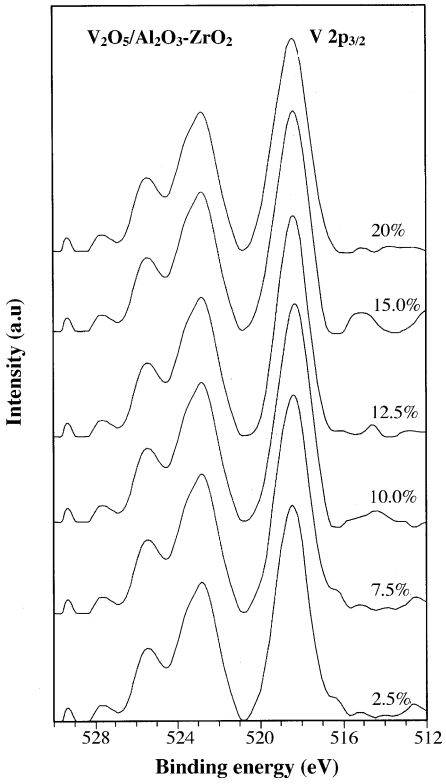

Fig. 7. V 2p XPS of V_2O_5/Al_2O_3–ZrO_2 catalysts.

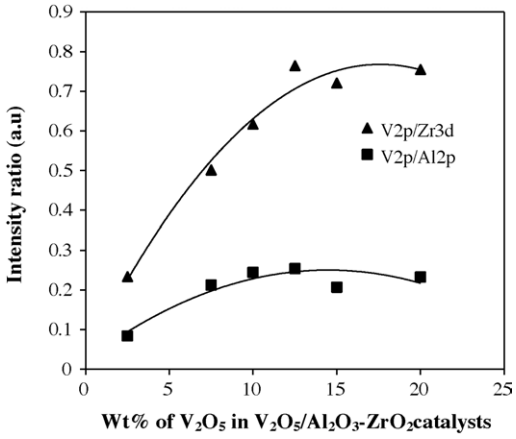

Fig. 8. XPS intensity ratio versus V_2O_5 loading for the V_2O_5/Al_2O_3–ZrO_2.

in calcined supported vanadia catalysts [39]. Only V (5+) is observed in calcined supported vanadia catalysts by XPS, when the sample is not artificially reduced by the measuring conditions. Traces of V (4+) are also present and not detected by XPS. It is well known that V (5+) does not have any unpaired electrons and no EPR signals where as V (4+) is EPR active. Thus, calcined supported vanadia catalysts possess V (5+) species and with trace amounts of V (4+) species [39,40].

The surface atomic ratios were calculated from the XPS peak intensity ratios, normalized by atomic sensitivity factors [41]. Fig. 8 indicates that there is a surface enrichment of V with respect to Zr or Al. At higher vanadia contents, the surface V/Zr and V/Al ratio remains practically constant or increases very little. This reveals that at 12.5 wt.% vanadia and above loadings there is a segregation of vanadium oxide. The relative dispersion of vanadium on the support surface also determined from XPS measurements of the V_2O_5/Al_2O_3–ZrO_2 catalysts presented in Table 4 and Fig. 8. The XPS data were quantified for V/Zr and V/Al atomic ratios. It is evident form Fig. 8 that V/Zr and V/Al atomic ratio is not proportional to the vanadia loading. Up to 12.5 wt.% monolayer loading, the increase in the atomic ratio is almost linear, which indicates a high dispersion of vanadia below monolayer loading. At higher loadings, the V/Al ratio is constant and no appreciable surface enrichment of V/Zr atomic ratios is observed. This confirms the formation of agglomerates and crystallites at higher vanadia loadings. These results are in agreement with the studies of Huuhtanen and Andersson [37] and confirm that at low vanadia loadings dispersion is high and at higher loadings the dispersion decreases. The activity of the catalysts in the ammoxidation of toluene to benzonitrile was also found to increase up to 12.5 wt.% loading and leveled off at higher loadings.

The DR-UV–vis spectra of V_2O_5/Al_2O_3–ZrO_2 catalysts are shown in Fig. 9. The charge transfer (CT) spectra of V^{5+} ions (d^0) were recorded between 200 and 800 nm for Al_2O_3–ZrO_2 supported VO_x catalysts containing 2.5–20 wt.% of V_2O_5. In all the catalysts the spectrum is dominated by two charge transfer (CT) bands of V^{5+} (d^0) at 288 and 367 nm (Fig. 9). The energy of oxygen → vanadium charge transfer absorption band, which is correlated with the minimum diffuse reflectance, is strongly influenced by the number of ligands surrounding the central vanadium ion. Thus, it can be used to obtain very useful information on the coordination of vanadium ions in different surface species

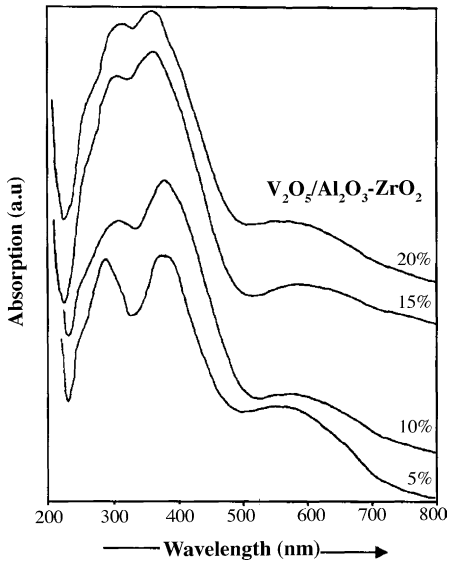

Fig. 9. UV–vis diffuse reflectance spectra of the V_2O_5/Al_2O_3–ZrO_2 catalysts.

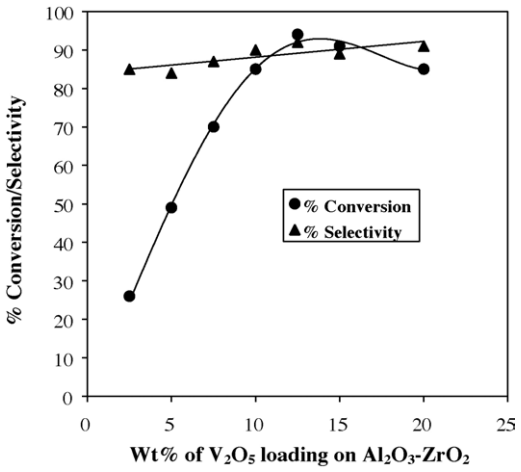

Fig. 10. Ammoxidation of toluene over various V_2O_5/Al_2O_3–ZrO_2 catalysts (reaction temperature 643 K).

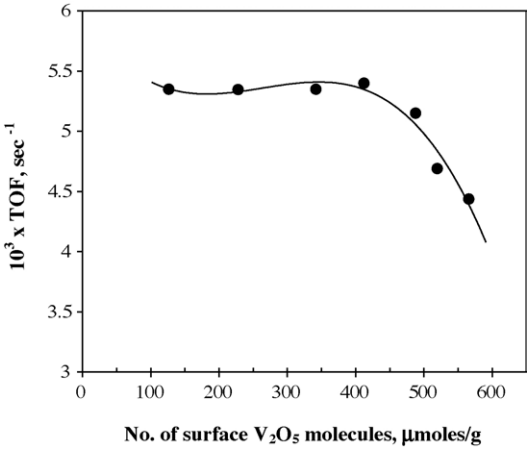

Fig. 11. Dependence of turn over frequency (TOF) on surface vanadia content.

[42,43]. The spectral features of the catalysts, consisting of an absorption band at 288 nm arise from the charge transfer in di- or oligo-meric structures formed by the condensation of monomeric species and V^{5+} ion in tetrahedral coordination [43]. The blue shift of this band has been observed from 288 to 311 nm with increase in vanadia loadings. In all the systems the charge transfer band at ~375 nm is due to V^{5+} ions coordinated by five oxygen ligands in the form of a square pyramidal [43].

The results of ammoxidation of toluene at 643 K over various V_2O_5/Al_2O_3–ZrO_2 catalysts are presented in Fig. 10. The conversion of toluene was found to increase with increase of vanadia loading up to 12.5 wt.% vanadia, and decreases at higher vanadia loadings. The decrease in activity of the catalysts beyond 12.5 wt.% is due to agglomeration of V_2O_5 micro crystallites or completion of monolayer. Thus, the findings of oxygen chemisorption and XPS results further support the catalytic properties. The selectivity of benzonitrile formation is found to be independent of vanadia content in the catalyst. In the present study the catalysts have been pre-reduced in hydrogen and thus the reduced surface contains V^{4+} stabilized on alumina–zirconia surface. Experiments were conducted to establish the effect of mass transfer limitations during the ammoxidation reaction. The mass transfer limitations were evaluated using the Madon and Boudart test [44,45]. The rate of ammoxidation increased proportionally with the weight of catalysts indicating absence of any mass transfer limitations during the reaction. The rate of conversion of toluene (at a reaction temperature of 643 K and molar ratio of toluene:NH_3:air = 1:13:26) has been expressed interms of rate of toluene molecules converted per second per surface of V_2O_5 molecule, which termed as turn over frequency (TOF). This has been calculated by considering the dispersion of V_2O_5 obtained from oxygen chemisorption at 643 K.

A plot of turn over frequency versus the surface vanadia content is shown in Fig. 11. The TOF was found to be almost constant ($\approx 5.35 \times 10^{-3}\ S^{-1}$) up to 10 wt.% V_2O_5 and decreases at higher vanadia loadings. Up to 10 wt.% V_2O_5 loading, per site activity (constant TOF) is constant with increase in surface vanadia sites. The decrease in TOF beyond 10 wt.% V_2O_5 loading indicates the formation of crystalline V_2O_5 particles.

4. Conclusions

The Al_2O_3–ZrO_2 binary oxide is an interesting support to investigate the dispersion of vanadium oxide and catalytic properties. The oxygen chemisorption results suggested that vanadium oxide is highly dispersed on Al_2O_3–ZrO_2 support at lower vanadia loadings and the dispersion decreases with increase in vanadia loadings. XPS results further support the above findings. XPS results indicated the presence of V^{5+} in all the catalysts and did not show any reducible species. TPR results indicated that the reducibility of vanadia decreases with increase of vanadia loading. Al_2O_3–ZrO_2 was found to be a competent support and it plays an important role in the enhancement of V_2O_5 activity in the ammoxidation of toluene.

Acknowledgements

KVRC Thanks Royal Society of Chemistry, UK for the award of RSC Journals grant for international authors. CHPK thanks Council of Scientific and Industrial research (CSIR), New Delhi for the award of Senior Research Fellowship (SRF).

References

[1] S. Park, R.J. Gorte, J.M. Vohs, Appl. Catal. A: Gen. 200 (2000) 55.
[2] A. Martin, B. Lucke, Catal. Today 57 (2000) 61.
[3] K.V.R. Chary, G. Kishan, T. Bhaskar, Ch. Sivaraj, J. Phys. Chem. 102 (1998) 6792.

[4] P. Cavani, F. Cavani, I. Manenti, F. Trifiro, Catal. Today. 1 (1987) 245.
[5] A. Andersson, S.T. Lundin, J. Catal. 58 (1979) 383.
[6] P. Cavalli, F. Cavani, I. Manenti, F. Trifiro, Ind. Eng. Chem. Res. 26 (1987) 639.
[7] A. Andersson, S.T. Lundin, J. Catal. 58 (1979) 383.
[8] A. Andersson, P. Jan-Olov Bovin Walter, J. Catal. 98 (1986) 204.
[9] G.T. Went, L.J. Leu, A.T. Bell, J. Catal. 134 (1992) 479.
[10] N.K. Nag, F.E. Massoth, J. Catal. 124 (1990) 127.
[11] C.L. Pieck, S. del Val, M. Lopez Granados, M.A. Banares, J.L.G. Fierro, Langmuir 18 (2002) 2642.
[12] K.V.R. Chary, B.M. Reddy, N.K. Nag, V.S. Subrahmanyam, C.S. Sundanda, J. Phys. Chem. 88 (1984) 2622.
[13] J.L. Lakshmi, N.J. Ihasz, J.B. Miller, J. Mol. Catal. A: Chem. 165 (2001) 199.
[14] A.W. Stobbe-Kreemers, G.C. Van Leerdam, J.P. Jacobs, H.H. Brongersma, J.J.F. Scholten, J. Catal. 152 (1995) 130.
[15] K.V.R. Chary, G. Kishan, J. Phys. Chem. 99 (1995) 14424.
[16] A. Adamski, Z. Sojka, K. Direk, M. Che, Solid State Ionics 117 (1999) 113.
[17] H. Eckert, I.E. Wachs, J. Phys. Chem. 93 (1989) 6796.
[18] R. Kozlowski, R.F. Pettifer, J.M. Thomas, J. Phys. Chem. 87 (1983) 5176.
[19] T. Tanaka, H. Yamashita, R. Tsuchitani, T. Funabiki, S. Yoshida, J. Chem. Soc. Faraday Trans. 1 84 (1988) 2987.
[20] H. Schaper, E.B.M. Doesburg, L.L. Van Reigen, Appl. Catal. A: Gen. 7 (1983) 211.
[21] A. Sahibed-Dine, B. Bouanis, K. Nohair, M. Bensitel, Ceram. Int. 28 (2002) 159.
[22] S.C. Farmer, A. Sayir, Eng. Fract. Mech. 69 (2002) 1015.
[23] J.M. Dominguez, J.L. Hernandez, G. Sandoval, Appl. Catal. A: Gen. 197 (2000) 119.
[24] C. Larese, J.M. Campos-Martin, J.J. Calvino, G. Blanco, J.L.G. Fierro, Z.C. Kang, J. Catal. 208 (2002) 467.
[25] I. Peeters, A.W. Denier van der Gon, M.A. Reijme, P.J. Kooyman, A.M. de Jong, J. Van Grondelle, H.H. Brongersma, R.A. Van Santen, J. Catal. 173 (1998) 28.
[26] F. Arena, F. Frusteri, A. Parmaliana, Appl. Catal. A 176 (1999) 189.
[27] F.J. Gil-Llambias, A.M. Escuday, J.L.G. Fierro, A. Lopez- Agudo, J. Catal. 95 (1985) 520.
[28] M.A. Eberhardt, A. Proctor, M. Houalla, D.M. Hercules, J. Catal. 160 (1996) 27.
[29] G. Meunier, B. Mocaer, S. Kasztelan, L.R. Le Coustumer, J. Grimblot, J.P. Bonelle, Appl. Catal. 21 (1986) 329.
[30] I.E. Wachs, Catal. Today 27 (1996) 437.
[31] K.V.R. Chary, G. Kishan, K.V. Narayana, T. Bhaskar, J. Chem. Res. (S) (1998) 314.
[32] M.M. Koranne, J.G. Goodwin Jr., G. Marcelin, J. Catal. 148 (1994) 369.
[33] H. Bosch, B.J. Kip, J.G. van Ommen, P.J. Gellings, J. Chem. Soc. Faraday Trans. 1 80 (1984) 2479.
[34] F.J. Roozeboom, M.C. Mittlemeijer-Hazeleger, J.A. Mouljin, M. Medema, V.H.J. de beer, P.J. Gellings, J. Phys. Chem. B. 84 (1980) 2783.
[35] C.R. Dias, M.F. Portela, G.C. Bond, J. Catal. 157 (1995) 344.
[36] G.C. Bond, Appl. Catal. A. 157 (1997) 91.
[37] J. Huuhtanen, S.L.T. Andersson, Appl. Catal. 98 (1993) 159.
[38] C.D. Wagner, W.M. Riggs, I.E. Davis, J.F. Moulder, in: G.E. Muilenberg (Ed.), Handbook of X-ray Photoelectron Spectroscopy, Perkin-Elmer Corporation, Minnesota, 1978.
[39] G.C. Bond, J.C. Vedrine, Catal. Today 27 (1996) 437.
[40] I.E. Wachs, B.M. Weckhuysen, Appl. Catal. A: Gen. 157 (1997) 67.
[41] C.D. Wagner, L.E. Davis, M.V. Zeller, J.A. Taylor, R.H. Raymond, L.H. Gale, Surf. Interface Anal. 3 (1981) 211.
[42] G. Centi, S. Perathoner, F. Trifiro, A. Aboukais, C.F. Aissi, M. Guelton, J. Phys. Chem. 96 (1992) 2617.
[43] M. Schraml-Marth, A. Wokaum, M. Pohl, H.L. Krauss, J. Chem. Soc. Faraday. Trans. 87 (1991) 2635.
[44] R.J. Madon, M. Boudart, Ind. Eng. Chem. Fund. 21 (1982) 438.
[45] U.K. Singh, M.A. Vannice, Appl. Catal. A: Gen. 213 (2001) 1.